proceedings

MDPI

Proceedings

Numerical prediction with high resolution mesoscale model and instrumental observation of wind conditions above city†

Alexander Starchenko [1,2,*], Lubov KIzhner [1], Elena Shelmina [1,3], Sergei Odintsov [2,1], Sergei Prokhanov [1], Evgeniy Danilkin [1,2]

[1] National Research Tomsk State University, Russia, 634050; kdm@mail.tsu.ru (L.K.); viking@math.tsu.ru (S.P.); ugin@math.tsu.ru (E.D.)
[2] V.E. Zuev Institute Atmospheric Optics SB RAS, Russia, 634055; odintsov@iao.ru (S.O.)
[3] Tomsk State University of Control Systems and Radioelectronics, Russia, 634055; eashelmina@mail.ru (E.S.)
* Correspondence: starch@math.tsu.ru (A.S.)
† Presented at the 4th International Electronic Conference on Atmospheric Sciences, 16-31 July 2021;

Abstract: The meteorological situations in Tomsk, accompanied by the occurrence of weak (less than 1 m/s) and strong winds (leading to the occurrence of wind gusts above 11 m/s), are considered. To study these phenomena, the meteorological equipment of the RESC 'Atmosphere' (Research Equipment Sharing Center of the IAO) and numerical mesoscale meteorological and photochemical models developed at TSU, were used. For light wind conditions, the TSUNM3 meteorological model confirmed the periods of the day when the observed wind velocity did not exceed 1 m / s. For strong wind conditions, the calculated wind velocity values change synchronously with the measured values.

Keywords: mesoscale model TSUNM3, calm wind conditions, urban air quality, strong wind prediction, observations RESC 'Atmosphere'

1. Introduction

Wind affects all industries: on the one hand, it determines the load on buildings and other structures (especially high-rise ones); on the other hand, it causes cooling effect, especially at low temperatures [1]. In addition, wind speed and direction determine air exchange and thus affect ecology of the region. The wind regime has a decisive influence on the dispersion of pollutants in the atmosphere. Areas of higher concentrations of pollutants are created in leeward areas relative to the sources of emissions.

With weak winds, the greatest air pollution is observed, and visibility deteriorates. Strong winds, on the contrary, ventilate a territory well, but create additional dynamic loads on buildings and structures. It is known that there is interrelation between seasonal changes in pollutants and the repeatability of the wind speed of 0-1 m/s. An increase in the number of weak winds in the annual course is accompanied by an increase in the average monthly concentrations of nitrogen oxides, carbon oxide and sulfur dioxide. The highest correlation between these values is found in the cities with the predominance of low emission sources, as well as where weak winds are observed in a large layer and elevated inversions are frequent. Depending on the wind speed, two peaks of urban air pollution are detected: when the wind is relatively weak (0-1 m/s) – with emissions from low sources and when the wind is 5-6 m/s – with emissions from high sources. At wind speeds of 2-3 m/s, there is a relative decrease in the concentration of pollutants [2].

The formation of atmospheric air pollution in cities depends on many factors [1]. Emissions from industrial enterprises, vehicles and meteorological conditions are the most important ones. Inversion in the atmosphere is an important criterion of adverse weather conditions. The lower the source of pollution is and the closer the base of the

Citation: Lastname, F.; Lastname, F.; Lastname, F. Title. *Proceedings* **2021**, *65*, x. https://doi.org/10.3390/xxxxx

Received: date
Accepted: date
Published: date

inversion to the source is, the greater the concentration of pollutants in the surface layer is. As wind speed decreases, pollutant concentration increases. The concentration of harmful pollutants increases when fogs accumulate pollutants and form substances of increased toxicity.

Currently, a large number of works are devoted to the study of the relationship between the level of air pollution from the direction and velocity of the wind. The authors of [3] devoted their work to the study of the influence of wind direction and velocity on the transfer of pollutants from road transport into the atmosphere. The study was carried out using a mobile laboratory in an urban area. The authors considered three spatial scales covering typical transport phenomena observed in urban environments: microscale (several tens of meters), medium (several hundred meters), and quarter-scale (several kilometers). Considering the micro-scale measurements, it has been found that the concentration of pollutants can be significantly influenced by wind direction, which results in a higher concentration of pollutants in the leeward lane, even on a small carriageway. In medium-scale experiments, an exponential decrease in the concentration of pollutants was observed with an increase in wind velocity and a change in wind direction. When examining measurements on a large scale (~ 15 km) over 14 days, it was found that the average concentration of pollutants on the road decreases as the prevailing wind velocity increases on a scale of the neighborhood to values above 2.0 m/s. Thus, the authors concluded that the concentration of emissions from road transport along highways has a pronounced negative linear dependence on wind velocity. Therefore, when examining the quality of atmospheric air, wind velocity is important not only on the ground, but also on the road or near a linear source. This is important to understand in order to interpret the measured data obtained on different days. Otherwise, it would be very difficult to find out the reasons for the large difference in concentration values at different times and under different weather conditions.

The understanding of how wind speed affects ground–level air pollution concentrations is relatively well established [4, 5]. Low wind speeds deteriorate air quality with respect to pollutants emitted near the ground due to restricted air ventilation. Stagnant atmospheric conditions with calm, clear weather often lead to stable atmospheric stratification which can transform into strong nocturnal temperature inversions due to rapid surface cooling. The resulting restriction in vertical air mixing near the surface consequently leads to poor air quality.

The work [6] indicates that cities in which there is a high surface wind speed have a lower percentage of cases of COVID-19. Results here suggest that high concentrations of air pollutants, associated with low wind velocities, may promote a longer permanence of viral particles in polluted air of cities, thus favouring an indirect means of diffusion of the novel coronavirus (SARS-CoV-2), in addition to the direct diffusion with human-to-human transmission dynamics.

The purpose of this work is to use the instrument base of the RESC "Atmosphere" and the mesoscale high-resolution (1km) meteorological model TSUNM3 [7] to predict the development of extreme weather events in Tomsk and the Tomsk region caused by strong (more than 11 m/s) and weak winds (up to 1 m/s).

Tomsk is the oldest city in Siberia, the center of the Tomsk region, an educational, scientific and cultural city, the population of which with its suburbs is about 800,000 people. Tomsk is located in the east of Western Siberia on the banks of the Tom River (56.5 N, 85.0 E). The climate is transitional from European temperate continental to Siberian sharply continental. Extreme temperatures are -55 °C in January and + 35 °C in July.

The relief of the city and its environs is not uniform. The city is located mainly on the high right bank of the river at the height of the Tom, 60 km from its confluence with the Ob River. The central part of the city is located at an altitude of about 120 m. To the east, the area rises, merging with the spurs of the Kuznetsk Alatau and the Salair Ridge (height up to 170 m). The left-bank part of Tom (western outskirts of the city) has an altitude of 80-110 m above sea level.

The vegetation in the surroundings is varied. Here the zones of taiga and forest-steppe converge. The presence of large forests in the vicinity of the city (aspen, birch, fir, cedar, pine) causes a significant macro-roughness of the surface, which contributes to a slight decrease in wind velocity compared to an open area. The difference in elevation and landforms in different areas of the city and its environs, the presence or absence of forest vegetation, the orientation of the Tom river valley affect the climate of the corresponding areas of the city, primarily on their temperature and wind regime.

2. Methods

2.1. Experimental setup and choice of cases

The choice of dates of 2019 for modeling was based on the results of observations obtained with the help of instruments of the RESC "Atmosphere" [8]. In particular, the "Meteo-2" ultrasonic weather stations located at the following points:

- IAO, roof of the laboratory of the Institute of Atmospheric Optics of the SB RAS; measurement level is 17 m above the underlying terrain and 5 m above the roof level, urban land.

- BEC, Basic Experimental Complex of IAO of SB RAS; measurements at heights of 5 m ("BEC-5") and 10 m ("BEC-10"), natural landscape.

Fig. 1 shows a map of the territory for which the calculation was performed, indicating landscape types with elevations above sea level (m) and the location of observation points.

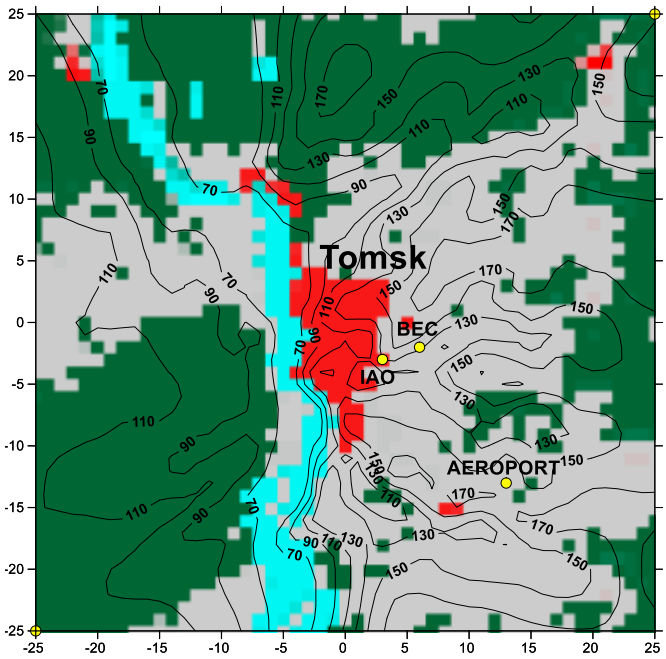

Figure 1. Relief of the study area, indicating the location of observation points. Blue color corresponds to the location of the water surface, green - forest, gray - insignificant vegetation. The position of the urban land use category is marked in red. Tomsk city is located in the center. Yellow circles mark the locations of observation points IAO, BEC, AEROPORT. Area size in kilometers.

2.1.1. Weak wind

Meteorological parameters averaged over a 10-minute time interval were used for the analysis (initial experimental data were obtained approximately 10 times per second). The choice of episodes with "calm conditions" was made by selecting those cases when the horizontal wind speed (V_h) was simultaneously less than 1 m/s at all observation points (IAO, BEC-5, BEC-10) in comparable 10-minute time intervals. At the same time,

the duration of such periods should have been at least 3 hours. The choice of the "3 hour" interval was made on the assumption that a weak wind or calm air should lead to a significant accumulation of pollutants in the surface layer of the atmosphere. For the period from 01.01.2019 to 31.10.2019, there were 17 such episodes. They occurred mainly in the warm season (March – May, July – September).

As a result, time intervals related to the category of "long calms" were identified according to the given scheme. The most striking cases were observed on 18.03.2019 (03:35-09:35), 23.07.2019 (03:05-08:55), 08.08.2019 (01:55-07:35), 12.08.2019 (02:35-07:15), 20.08.2019 (03:15-08:45), 05.09.2019 (05:35-08:25).

2.1.2. Strong wind

The average values of the horizontal wind speed V_h and the kinetic energy of turbulence E_k, which determines wind gustiness in each 10-minute interval at all observation points, were calculated for the specified period (01.01–31.10.2019) based on the obtained experimental data. Based thereon, the value [9] was calculated

$$G = V_h + 3\sqrt{E_k}, \quad (1)$$

which characterizes the "general level" of wind speed in the interval and is related to the number of possible predictors of wind gusts. The choice of episodes with "strong wind gusts" was made by selecting those cases when the G values simultaneously exceeded the level of 11m/s at all observation points in comparable 10-minute intervals. This level was selected based on the cumulative distribution function G for the specified period (99.5%). We selected 12 days when there were cases of G>11 m/s (only the dates and months of 2019 are specified): 26.04, 28.04, 29.04, 30.04, 18.05, 19.05, 20.05, 25.05, 26.05, 20.09, 24.09, 29.10. These cases also relate mainly to the warm period of the year.

2.2. TSUNM3 model description

The TSUNM3 model uses a system of non-hydrostatic equations of motion, heat, and mass transfer in the troposphere and in the upper soil layer [7]. TSUNM3 forecasts the components of wind speed and temperature and humidity characteristics in the atmospheric boundary layer at 50 vertical levels (up to 10,000 m) above the territory of 150×150 km and a nested area with a base of 50x50 km (grid step of 1 km with the center in the city of Tomsk). TSUNM3 takes into account the behavior of the following atmospheric processes:

- turbulent mixing in the atmospheric boundary layer, the nature of which is significantly affected by changes in the temperature of the underlying surface;
- radiation factors due to the influence of short-wave and long-wave radiation in the studied layer of the atmosphere taking into account the scattering and attenuation of radiation in a clear sky, absorption of radiation by water vapor, absorption and reflection by clouds;
- formation of raindrops, clouds, snow, ice particles and pellets in the atmosphere in accordance with the WSM6 microphysics of moisture scheme [10];
- turbulent exchange of momentum, heat, and moisture with the underlying surface;
- heating of the underlying surface by penetrating short-wave solar radiation and its cooling by long-wave radiation during the hours of darkness.

Initialization of the TSUNM3 model and supplying it with lateral boundary conditions is carried out based on a numerical weather prediction by the SL-AV [11] operational global model of the Hydrometeorological Center of the Russian Federation.

The non-stationary Eulerian chemical transport model (CTM) was used to calculate the formation and dispersion of pollutants in the atmosphere. The governing equations, along with the non-stationary term, contain terms that represent horizontal and vertical advection and turbulent diffusion, wet deposition, and source terms that model the emissions of primary air pollutants and their chemical reactions [12].

$$\frac{\partial C_i}{\partial t}+\frac{\partial UC_i}{\partial x}+\frac{\partial VC_i}{\partial y}+\frac{\partial WC_i}{\partial z}= \\ =\frac{\partial}{\partial x}\left(K_{xy}\frac{\partial C_i}{\partial x}\right)+\frac{\partial}{\partial y}\left(K_{xy}\frac{\partial C_i}{\partial y}\right)+\frac{\partial}{\partial z}\left(K_z\frac{\partial C_i}{\partial z}\right)-\sigma_i C_i+S_i+R_i, i=1,..,n_s. \quad (2)$$

$$-Lx/2 \le x \le Lx/2, -Ly/2 \le y \le Ly/2, h(x,y) \le z \le H, 0 \le t \le T,$$

where C_i is the concentration of the i-th component of the pollutant, U, V are the components of the vector of horizontal wind speed, W is the vertical wind velocity, S_i is the source term representing emissions of pollutant components in the atmosphere due to the elevated point and the linear land-based sources, R_i describes the formation and transformation of substance due to the chemical and photochemical reactions involving pollutant components, σ_i is the rate of wet deposition of pollutants, n_s is the number of chemical components of pollutant whose concentrations were modelled, x, y are horizontal coordinates, the Ox axis is directed eastwards, the Oy axis is directed northwards, z is the vertical coordinate, t is time, and T is the modeling period. The computational domain represents a parallelepiped, Lx, Ly are the horizontal dimensions of the domain, H is the height of the computational domain, and h(x,y) is the terrain height above sea level.

To describe chemical and photochemical reactions a kinetic scheme derived from a combination of two well-tested reduced chemical reaction mechanisms [13, 14] were applied. The model calculates the concentrations of such impurity components as carbon monoxide, sulfur dioxide, nitrogen monoxide and dioxide, hydrogen peroxide, etc.

3. 3. Results and discussion

The results of calculations of the surface wind speed at an altitude of 10m, performed with the use of the TSUNM3 model, for two positions corresponding to the location of the IAO and BEC stations (Fig.1) are represented below. The calculated data is compared with the observations at the IAO and BEC stations for the selected dates (see Sec. 2).

3.1. Weak winds

Figure 2 shows graphs of changes in the average velocity modulus measured at the IAO and BEC sites and predicted values of this parameter at a height of 10m with the use of the TSUNM3 model for the selected modeling dates (see Sec 2.1.1). The figures show that the model calculations correspond fairly well to the observation results. Indeed, the observed periods of time during the considered day when the wind speed at the observation points decreased below 1m/s are almost always confirmed by calculations. So, on July 23, 2019, it was observed at 03:05-08:55; August 8, 2019 - at 01:55-07:35; August 20, 2019 - at 03:15-08:45; September 5, 2019 - at 05:35-08:25; March 18, 2019 - at 03:35-09: 35. The time is local. Of all the modeled cases, the TSUNM3 model did not predict the decrease in the surface wind speed only on August 12, 2019 from 02:35 to 07:15. The predicted speed values at an altitude of 10m had values from 1 to 2 m/s during this time period.

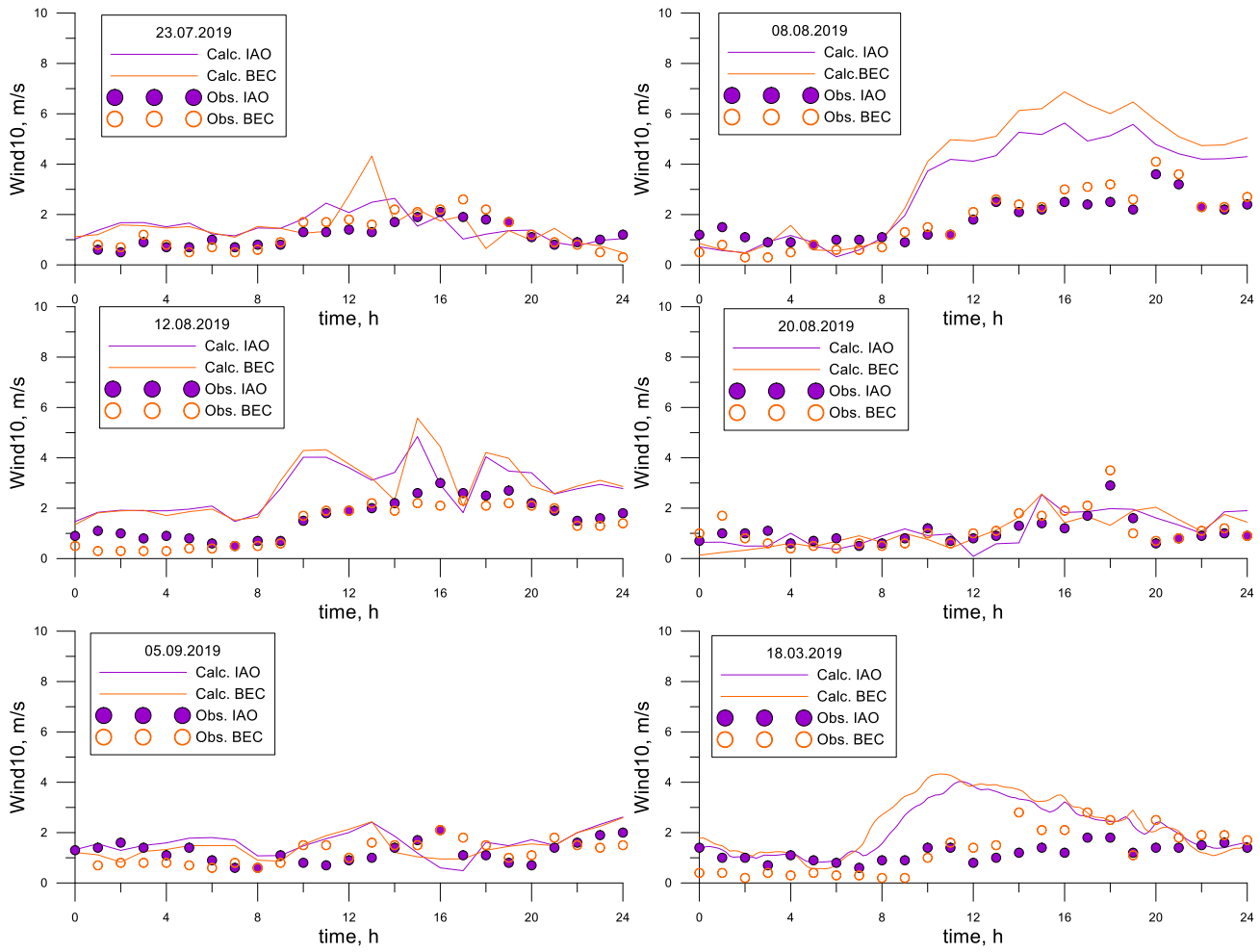

Figure 2. Calculated and measured change in the surface wind speed modulus during the day for the specified dates.

Numerical predictions were made using the developed CTM model (2) to demonstrate the influence of a weak wind on air quality in the city. The calculations were performed at the same intensity of elevated point sources and linear (automobile roads) sources located in the considered area. The intensity of the point and line sources corresponded to the annual emissions of the main pollutants in the Tomsk region for 2019. Changes in the normalized vehicle emission intensity $I_{Vehicle}$ during each calculation day were modeled according to the following law:

$$I_{Vehicle}(t_h)) = \begin{cases} 0,05 + 0,95\sin(\pi(t_h - 6)/18), t_h \in [6,24], \\ 0,05, t_h \notin [6,24], \end{cases} \quad (3)$$

Here t_h is local time in hours. According to this formula, the highest intensity of vehicle emissions is modeled around 15 o'clock local time. The vehicle emission intensity is minimal from 0 to 6 a.

When using the results of calculations obtained based on the CTM model (2), a qualitative indicator was considered to assess the air quality above the considered area, i.e. the Air Pollution Index (API). The API values are calculated based on the predicted concentrations of CO, SO2, NO2, NO, and O3 with the following equation.

$$API = \sum_{i=1}^{n} \left(\frac{C_i}{C_{i\infty}} \right)^{a_i}, \quad (4)$$

where C_i is the concentration of the i-th substance, mg/m3, values of $C_{i\infty}$, mg/m3, and the dimensionless constants a_i are presented in Table 1.

Table 1. The constants for calculating the Air Pollution Index (4)

Constants in (4)	CO	SO_2	NO_2	NO	O_3
$C_{i\infty}$	5.0	0.5	0.2	0.40	0.16
a_i	0.9	1.0	1.3	1.0	1.7

The API calculated with Equation (4) was recommended for the urban air quality assessment by The Federal Service for Hydrometeorology and Environmental Monitoring (Rosgidromet).

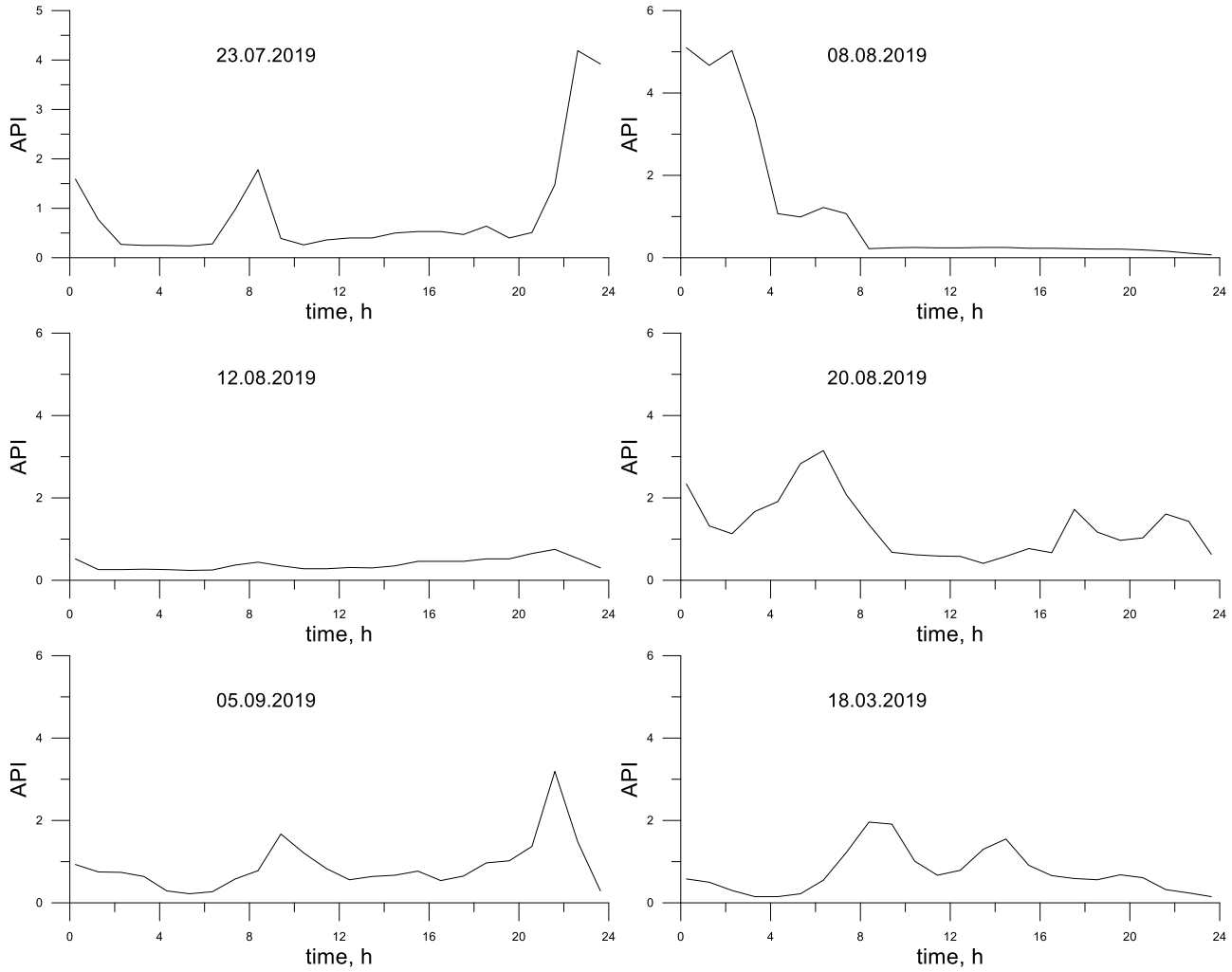

Figure 3. Calculated values of the Air Pollution Index at an altitude of 10m for the city center for selected modeling cases.

Fig. 3 shows the calculated API values. For the selected dates, the same-type clear or cloudy weather was observed without precipitation with medium- or upper-level clouds (the height of the lower boundary of clouds is more than 2 km). And on certain dates and periods, there was haze or fog. Figure 3 shows API graphs that can be used to determine how weak surface wind influences air quality. Model calculations fully confirmed the relationship of the considered parameters of the atmosphere. In addition, we obtained numerical increases in the API values above two for other time points of the modeled day, when calculations based on the mesoscale meteorological model showed low values of wind speed at an altitude of 10m. The deterioration of air quality with a decrease in

wind speed was particularly pronounced from 0 to 4 o'clock on August 8, from 4 to 8 on August 20, and less pronounced - around 8 o'clock on July 23, September 5 and March 18, 2019. On August 12, 2019, the calculations did not show an increase in API during the entire time of day, since the TSUNM3 model predicted the surface wind speed of 2 to 4 m/s at the points under consideration on that day. It is of interest, that the photochemical model predicted increased API values for the time periods that were not included in the chosen samples with calm air recommended in Sec. 2.1.1. For example, from 22 to 24 o'clock on July 23, from 00 to 02 o'clock on August 8, and about 22 o'clock on September 5, 2019. In the first two cases, low surface wind values were calculated. It should be noted that in these three periods of time, in addition to the weak wind, stable stratification of the atmosphere, which leads to the accumulation of pollutants near the earth's surface, could have an additional impact on the increase in the surface air pollution [1,2]. It is also interesting that increased API was accompanied by haze or fog, and there was a high relative humidity on three out of the six dates under consideration (there was haze at 01-04 o'clock on July 23, fog - at 03-05 o'clock; there was haze at 04 o'clock on August 20, fog - at 07-10 o'clock; there was haze at 07-10 o'clock on March 18). As is known, the formation of fogs is an additional factor that leads to an increase in the concentration of pollutants in the air.

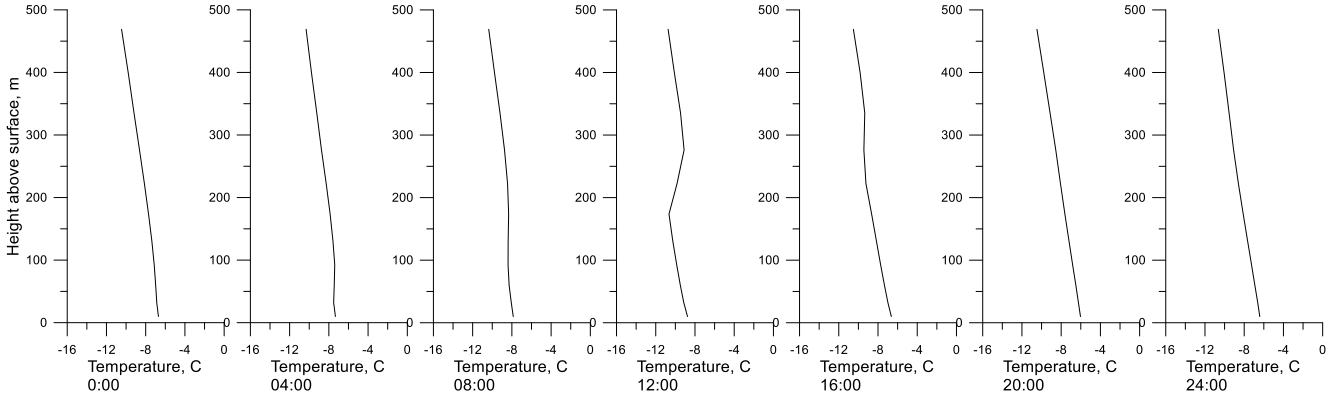

Figure 4. Vertical temperature profiles predicted with the TSUNM3 model for 18.03.2019. Local time.

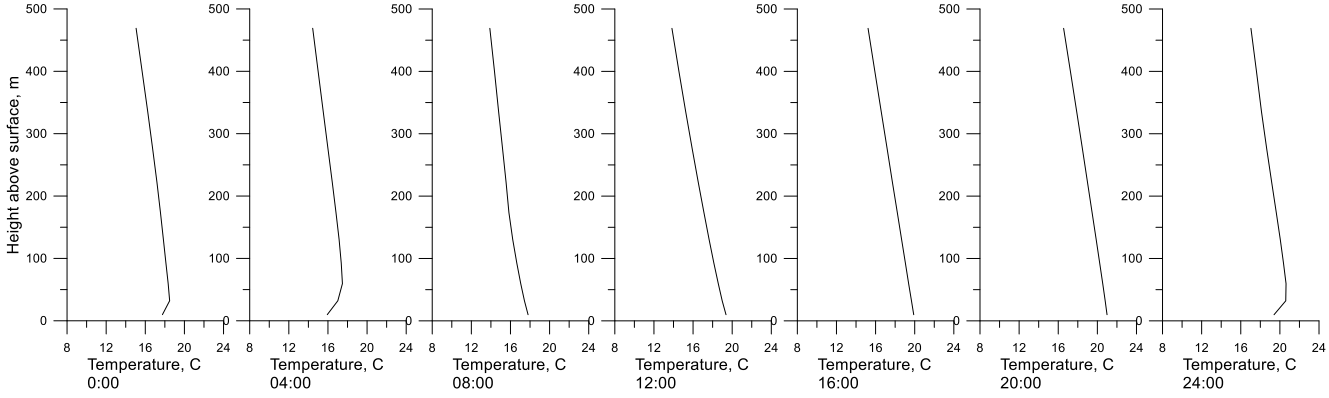

Figure 5. Vertical temperature profiles predicted with the TSUNM3 model for 8.08.2019. Local time.

Calculations of the vertical temperature profile in the 0-500 m layer were performed to assess the impact of the atmospheric stability on increasing pollution levels, The assessment of the vertical temperature profile showed that the considered dates are characterized by the presence of the surface inversion or isothermy at 00 and 04 o'clock, and surface or raised one at 08 o'clock. It was not observed at 12, 16, and 20 o'clock (except for the spring date of March 18, when inversion aloft in the 180-280 m layer was observed at 12 o'clock (Fig. 4,5). API increases were observed in the presence of inversion or iso-

thermy, either synchronously, or an increase in pollution was observed some time after the appearance of the inversion.

Table 2. The correspondence between the predicted vertical temperature profile and API (number of cases, percentages in brackets).

Inversion	API course		Total
	Increased (increase)	Not increased (not increasing)	
There is inversion, isothermy	13 (31)	7 (17)	20 (48)
No inversion, isothermy	0 (0)	22 (52)	22 (52)
Total	13 (31)	29 (69)	42 (100)

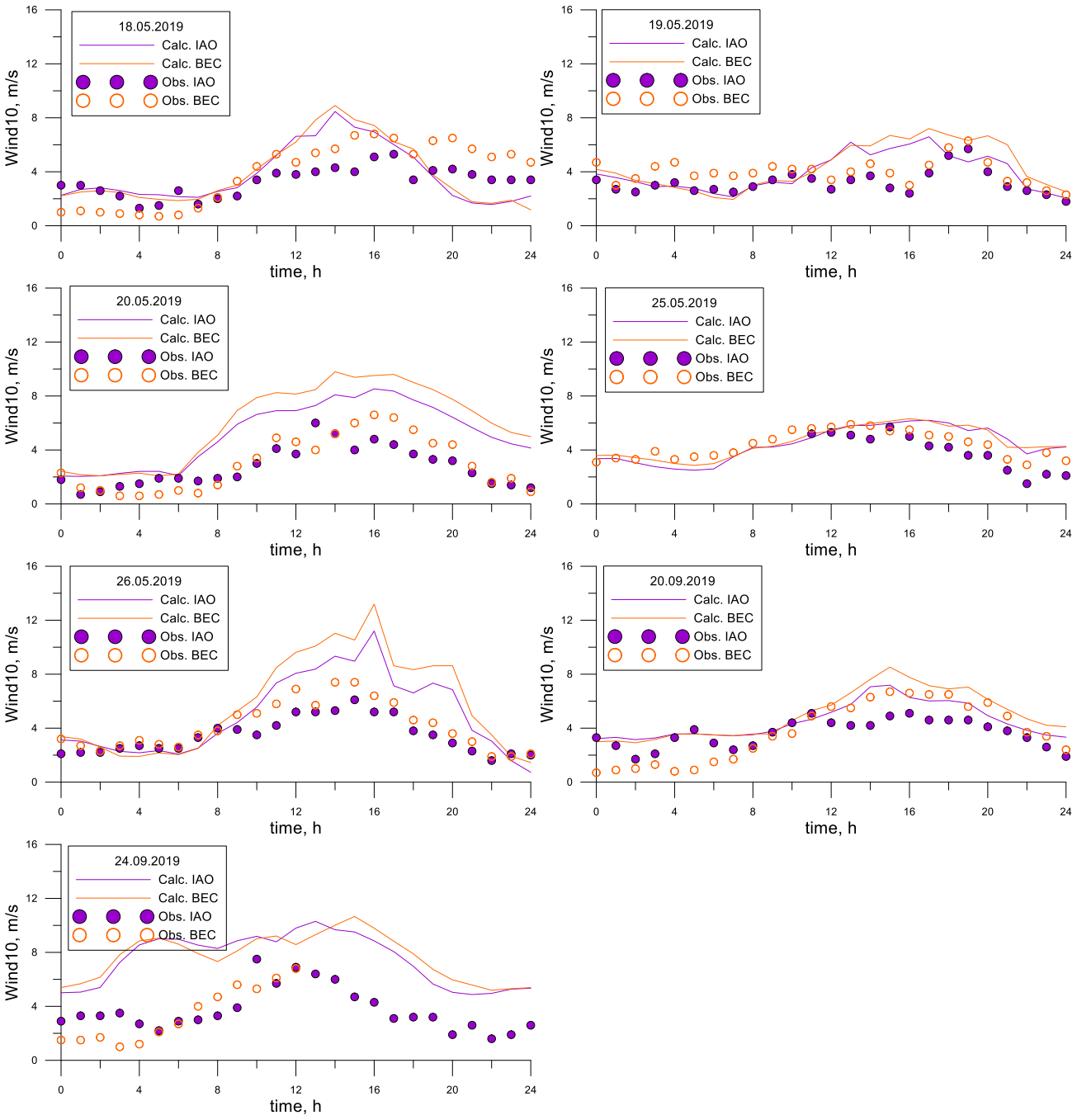

Figure 6. Diurnal variation of the measured (icons) and calculated (solid lines) surface wind speed in the selected points for the considered dates.

A table was compiled showing the relationship between the presence of inversion (isothermy) and increased (an increase of) API. Each case corresponds to the time when API and vertical temperature profile were calculated. The data is presented in table 2. So, in 83% of the cases, there is a direct relationship between the presence (absence) of inversion and the increase (non-increase) of API. In 17% of the cases, API did not increase if there was inversion. If there was no inversion, there was no increase in API observed.

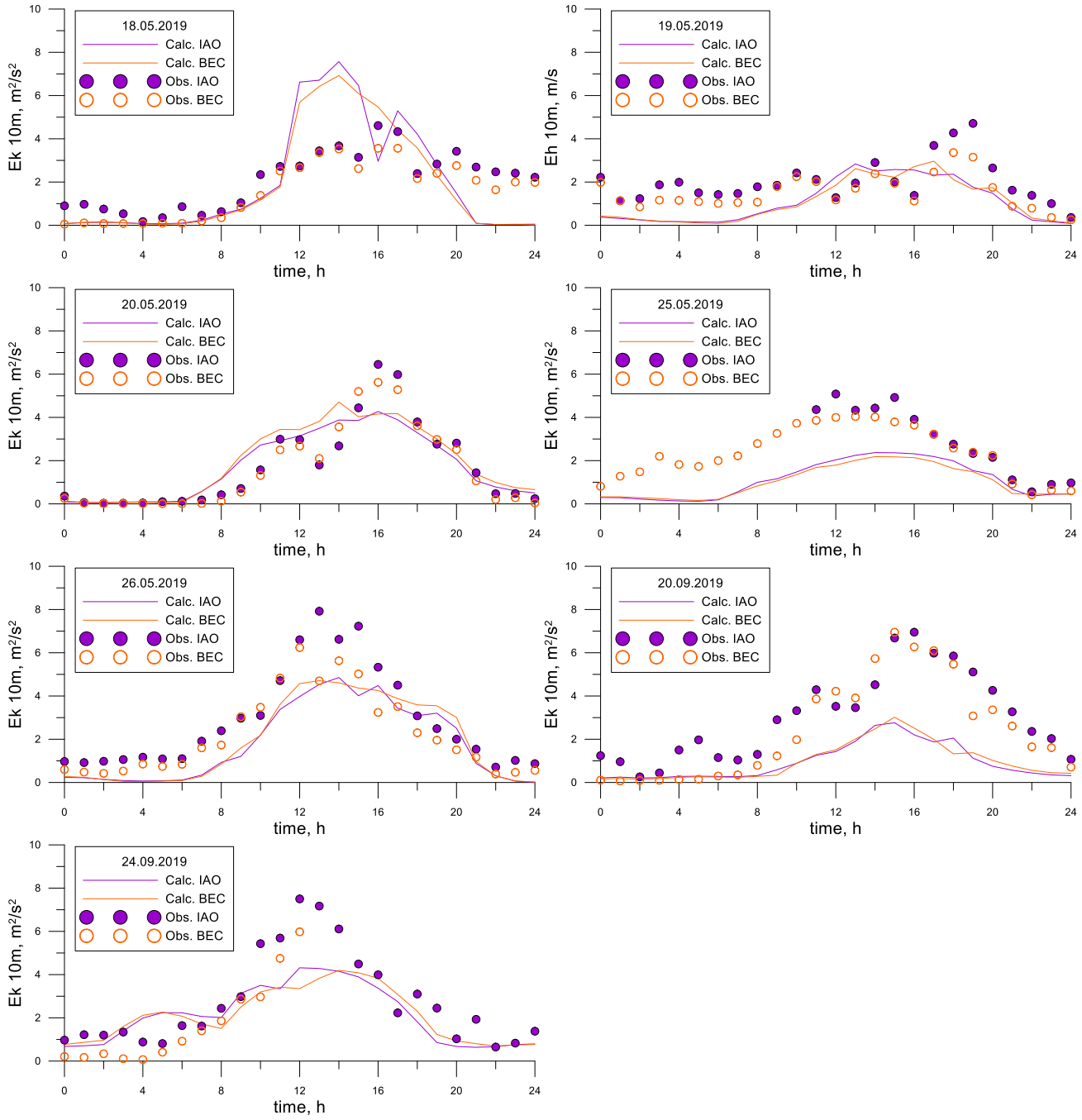

Figure 7. Diurnal variations of the measured (icons) and predicted (solid lines) turbulent kinetic energy near the surface in the selected points for the considered dates.

3.2. Strong winds

Figure 4 shows graphs of changes in the average velocity modulus V_h measured at the IAO and BEC sites and predicted values of this parameter at an altitude of 10m using

the TSUNM3 model for the selected modeling dates, when assessment by the formula (1) indicated high probability of wind gusts over 11m/s (see Sec. 2.1.2): 18.05, 19.05, 20.05, 25.05, 26.05, 20.09, 24.09.2019. It should be noted that the graphs show the average hourly measured values of wind speed V_h, so they are less than 11 m/s.

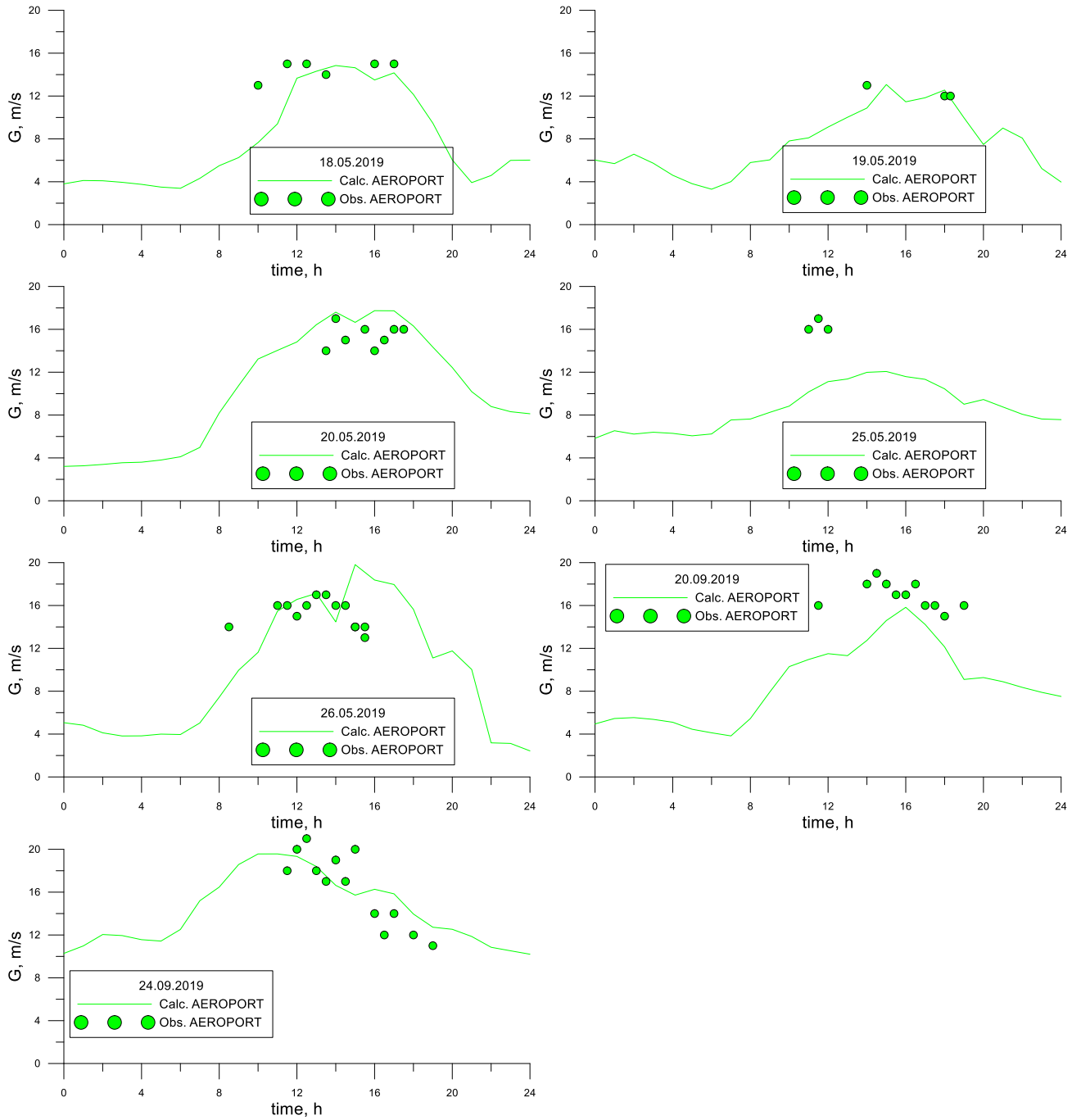

Figure 8. Diurnal variations of TSUNM3 predicted (solid line) G velocity (see (1) – wind gust scale) near the surface in the AEROPORT site for the considered dates. The green icons correspond to the time points when wind gusts over 11 m/s were recorded at the AEROPORT meteostation (Fig. 1).

Comparison of the calculation results with observations shows that, in general, the maximum values of the average wind speed are predicted at the time when they were observed (see Fig.6 and Sec.2.1.2). The meteorological model slightly overestimates the maximum value of the average speed obtained experimentally. Moreover, higher speed

values are more often predicted for the BEC point located near Tomsk outside the city than for the IAO point (urban area). Apparently, this is due to the different openness of the place (urban development in the center and natural landscape at the BEC point). It should also be noted that the position of the maximum values of experimental and calculated surface speeds corresponds to the forecasts of the meteorological service of the Tomsk airport (Fig. 8) for the periods of time when wind gusts reach more than 11 m/s (http://rp5.ru).

The model-calculated values of the kinetic energy of turbulence E_k correlate well with the measured values: small values of E_k are observed from midnight to 06-08 o'clock and after 22 o'clock, they do not exceed 2 m/s (Fig.7). During the day, with the development of convection, E_k increases and reaches maximum values in the period from 11-12 o'clock to 16-17 o'clock. The maximum calculated values are 4-8 m/s (in the center they are usually 1-2 m/s higher than at the BEC point), experimental values are 5-8 m/s. Model values of E_k can be higher or lower than the measured ones. Thus, high wind speeds are accompanied by increased gustiness.

Conclusions

Meteorological situations over the city of Western Siberia accompanied by weak (<1 m / s) and strong (> 11 m / s) surface wind were investigated with the help of ultrasonic meteorological stations "Meteo-2" of the RESC "Atmosphere" and a mesoscale model of numerical weather forecast with a horizontal resolution of 1 km TSUNM3.

The continuous use of weather stations from January, 1 to October, 30 of 2019 made it possible to identify periods when the surface wind speed for three hours at all observation points was less than 1m / s. For these dates of 2019, numerical simulations of weather conditions and air quality in the city were carried out. Comparison of calculations with observations showed that the TSUNM3 model in most cases confirms by calculations the duration and the very fact of weak wind conditions. However, in some cases, the TSUNM3 model overestimates the values of the surface wind speed in comparison with the observational data. Application of the developed model of atmospheric air quality confirmed the relationship between weak surface wind and deterioration of air quality in the city. This is especially shown in the combination of a weak wind with the conditions of stable stratification of the surface air layer.

Also, using the meteorological stations of the RESC "Atmosphere", episodes of the first ten months of 2019 were identified, when the scale of wind gusts estimated from observations exceeded 11 m / s at all observation points. For the selected dates, numerical weather modeling was carried out, which showed, in general, the correspondence of the measured and calculated values of the averaged velocity and turbulent kinetic energy of the surface wind. Using these values, the magnitude and duration of wind gusts were estimated. It was found that they correspond to the values and time of observations to wind gusts at the aviation meteorological station at the airport in Tomsk.

Author Contributions: Conceptualization, writing-review and editing, A.S.; investigation, L.K.; investigation, E.S.; resources, S.O.; software, S.P.; editing, E.D.

Funding: The work was supported by the Russian Science Foundation (project no.19-71-20042). Experimental data used for comparison with model calculations were obtained with the support of the Ministry of Education and Science of the Russian Federation (project no.AAAA-A17-117021310142-5).

Conflicts of Interest: The authors declare no conflict of interest.

References

1. Oke, T.R., Mills, G., Christen, A., Voogt, A. *Urban Climates*, Publisher: Cambridge University Press, 2017.
2. Zhuravlev G.G., Gorbatenko V.P., Gordov E.P. *Distribution of pollutants in the atmosphere and methods of their control*, 2013.
3. Kim, K.H., Lee, S.-B., Woo, D., Bae, G.-W. Influence of wind direction and speed on the transport of particle-bound PAHs in a roadway environment. *Atmospheric Pollution Research* **2015**, *6*, 1024-1034.

4. Grundstrom, M., Tang, L., Hallquist, M., Nguyen, H., Chen, D., Pleijel, H. Influence of atmospheric circulation patterns on urban air quality during the winter. *Atmospheric Pollution Research* **2015**, *6*, 278-285.
5. Jones, A.M., Harrison, R.M., Baker, J. The wind speed dependence of the concentrations of airborne particulate matter and NOx. *Atmospheric Environment* **2010**, *44*, 1682-1690.
6. Coccia, M. How do low wind speeds and high levels of air pollution support the spread of COVID-19? *Atmospheric Pollution Research* **2021**, *12*, 437-445.
7. Starchenko, A.V., Bart, A.A., Kizhner L.I., Danilkin, E.A. Mesoscale meteorological model TSUNM3 for the study and forecast of meteorological parameters of the atmospheric surface layer over a major population center. *Tomsk State University Journal of Mathematics and Mechanics* **2020**, *66*, 35-55.
8. Gladkikh, V.A., Makienko, A.E., Miller, E.A., and Odintsov, S.L. Study of the Atmospheric Boundary Layer Parameters under Urban Conditions with Local and Remote Diagnostics Facilities. Part 2. Air Temperature and Heat Flux. *Atmospheric and Oceanic Optics* **2011**, *23*, 280-287.
9. Byzova, N.L., Ivanov, V.N., Garger, E.K. *Turbulence in atmospheric boundary layer*; Publisher: Hydrometeoizdat, Russia, 1989; p. 263.
10. Hong, S.-Y., Lim, J.-O, J. The WRF single-moment 6-class microphysics scheme (WSM6). *J. of Korean meteorological society* **2006**, *42(2)*, 129-151.
11. Tolstykh, M.A., Fadeev, R.Yu., Shashkin, V.V., Goyman, G.S., Zaripov, R.B., Kiktev, D.B., Makhnorylova, S.V., Mizyak, V.G., Rogutov, V.S. Multiscale Global Atmosphere Model SL-AV: the Results of Medium-range Weather Forecasts. *Russ. Meteorol.Hydrol.* **2018,** *43*, 773-779.
12. Starchenko, A., Shelmina, E., Kizhner, L. Numerical Simulation of Meteorological Conditions and Air Quality above Tomsk, West Siberia. *Atmosphere* **2020**, *11*, 1-15. doi:10.3390/atmos11111148
13. Hurley, P.J. *TAPM V4. Part 1: Technical Description*. Publisher: CSIRO Marine and Atmospheric Research, Australia, 2008. doi:10.4225/08/585c175bc5884.
14. Stockwell, W.R., Goliff, W.S. Comment on «Simulation of a reacting pollutant puff, using an adaptive grid algorithm» by R. K. Srivastava et al. *J. Geophys. Res.* **2002**, *107(22)*, 4643–4650. doi:10.1029/2002JD002164